Electronic Supplementary Information

Magnetic Particle Ornamented Dual Stimuli Responsive Nanogel for Controlled Anticancer Drug Delivery

Pijush Mandal[a], Somnath Maji[b], Sudipta Panja[a], Om Prakash Bajpai[a], Tapas Kumar Maiti[b] and Santanu Chattopadhyay[a]*

[a]Rubber Technology Centre, Indian Institute of Technology, Kharagpur-721302, India

[b]Department of Biotechnology, Indian Institute of Technology, Kharagpur-721302, India

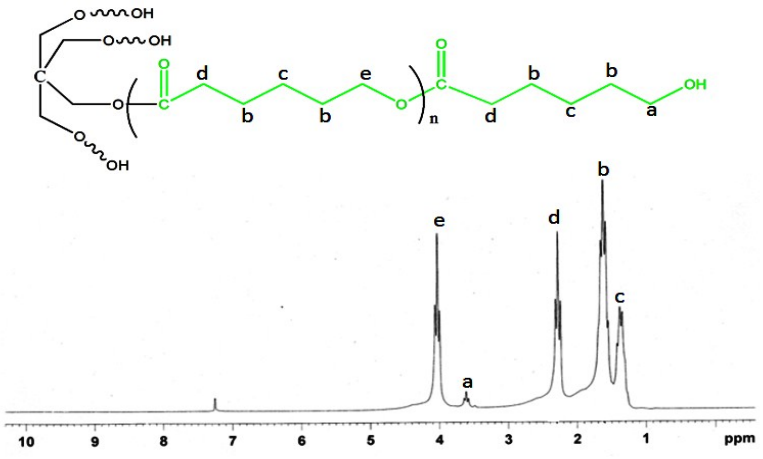

Figure S1: ^{1}H NMR spectrum of PE-PCL in $CDCl_3$

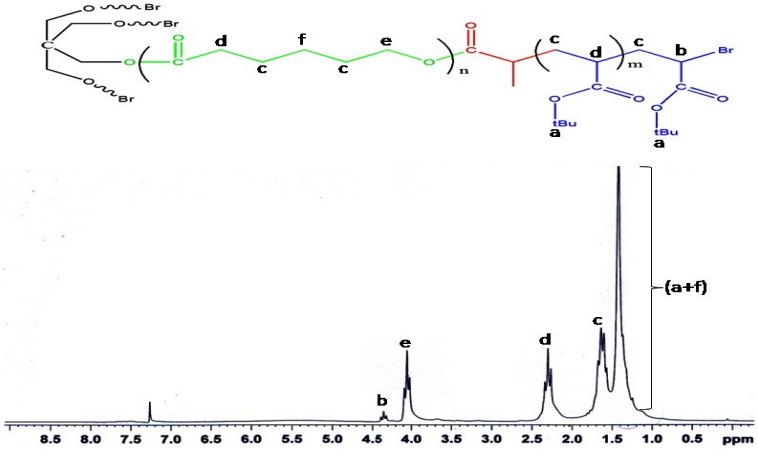

Figure S2: ^{1}H NMRspectrum of PE-PCL-P^{t}BA-Br in $CDCl_3$

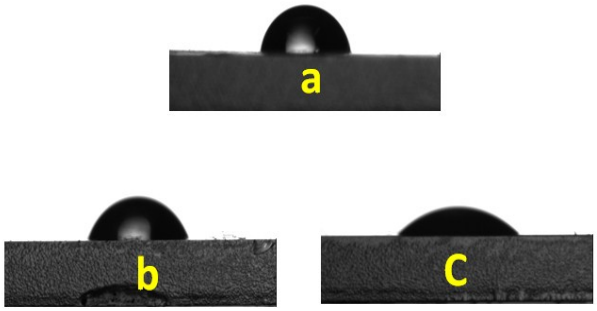

Figure S3: Water contact angle of sample (a) PE-$P(CL)_{20}$ (b) PE-$P(CL)_{20}$-b-$P(AA)_{180}$ (c) PE-$P(CL)_{20}$-b-$P(AA)_{229}$

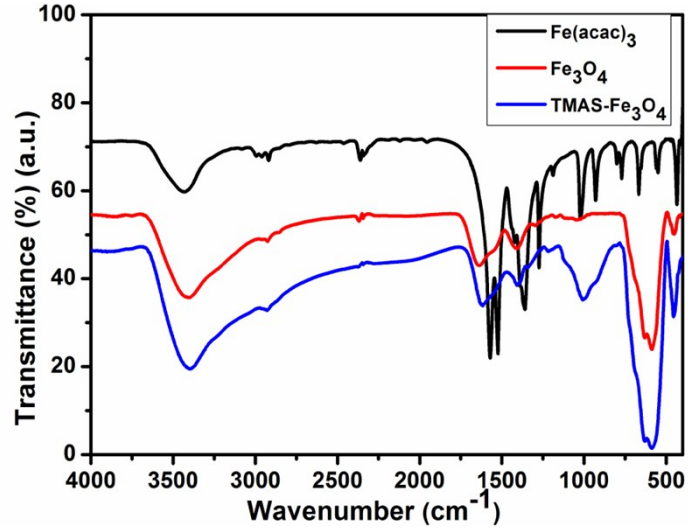

Figure S4: FTIR spectroscopy of $Fe(acac)_3$, Fe_3O_4, TMAS-Fe_3O_4

The stretching frequency at 667 cm^{-1} is associated with 'Fe-O' bond of the Iron (III) acetylacetonate. Interestingly, after the thermal treatment of $Fe(acac)_3$, the stretching band associated with 'Fe-O' (667 cm^{-1}) bond has been disappeared followed by the appearance of two new bands at 587 and 465 cm^{-1}. The band at 587 and 465 cm^{-1} are assigned to the stretching vibration of tetrahedral unit of FeO_4 and the vibration of octahedral unit of FeO_6 (intrinsic vibrations of ferrite), respectively. A comparative analysis of FTIR spectra for MNP's before and after the silane coating is also shown in Figure S1. In the FTIR spectrum of TMAS-Fe_3O_4 bands

at 1010 and 1570 cm^{-1} are corresponds to Si–O–Si stretching and bending vibration of primary amine, respectively [1]. Hence, the FTIR results suggest the successful synthesis of both the Fe_3O_4 and TMAS-Fe_3O_4.

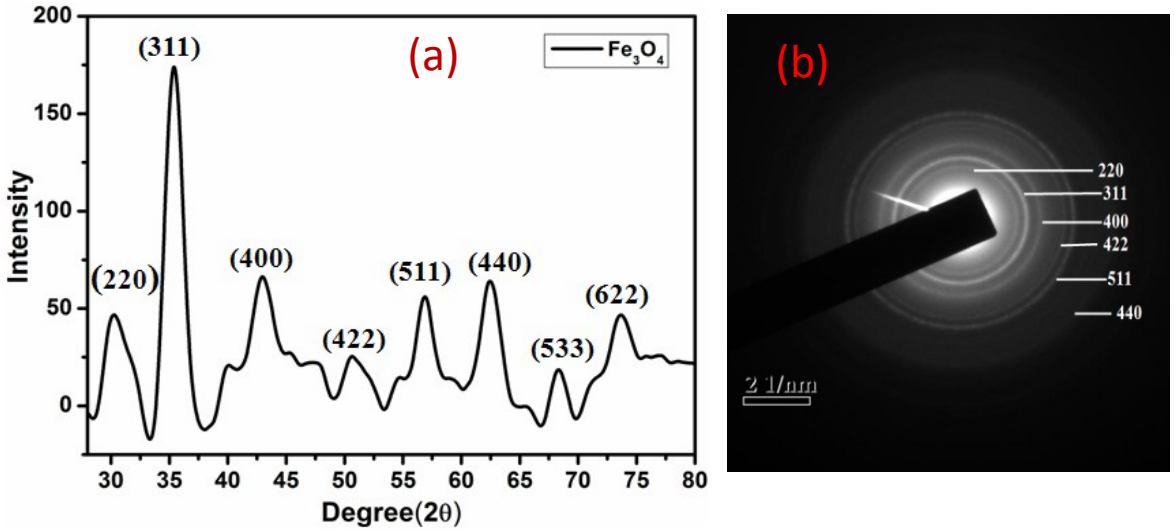

Figure S5: (a) X-ray diffraction pattern and (b) Selected area diffraction (SAED) pattern of pristine Fe_3O_4 nanoparticles

XRD measurement is valuable tool to determine the phase structure of nanoparticles. As shown in Figure S5a, the peaks are observed at 2θ = 30°, 35°, 43.2°,53°, 58.3°, 62° and 74.1° which represent the Bragg reflection from the (220), (311), (400), (422), (511), (440) and (622), respectively(obtained from JCPDS No. 10-0319). Typical XRD pattern reveals the inverse spinel cubic structure of MNPs.

This also supports the formation of the inverse spinel cubic phase of MNP as elucidated in the XRD section. The elemental analysis is one of the methods to confirm the chemical composition of the so formed MNP. Figure S6 (a) and (b) shows the typical EDS of the pristine and silane coated MNP, respectively. The analysis result show the peaks corresponding to two different oxidation states of Fe as well as the peak of silica (after modification). The appearance of the peaks Cu and C are assumed for the carbon coated Cu grid.

Morphological analysis of functionalized MNP

The bulk morphology, particle shape and size of the MNPs are visualized by HRTEM analysis. MNPs are nearly spherical in shape and average size is 5 nm. The pristine MNPs are forming some clusters because of their strong magnetic force (Figure1A). However, after coating with TMAS, a layer is formed around the particles (Figure 1B) which fairly reduces their cluster forming tendency. The modification of the MNPs with TMAS brings a huge number of hydrophilic '-NH_2' groups at the surface of TMAS-MNP which results in the increase of their colloidal stability.

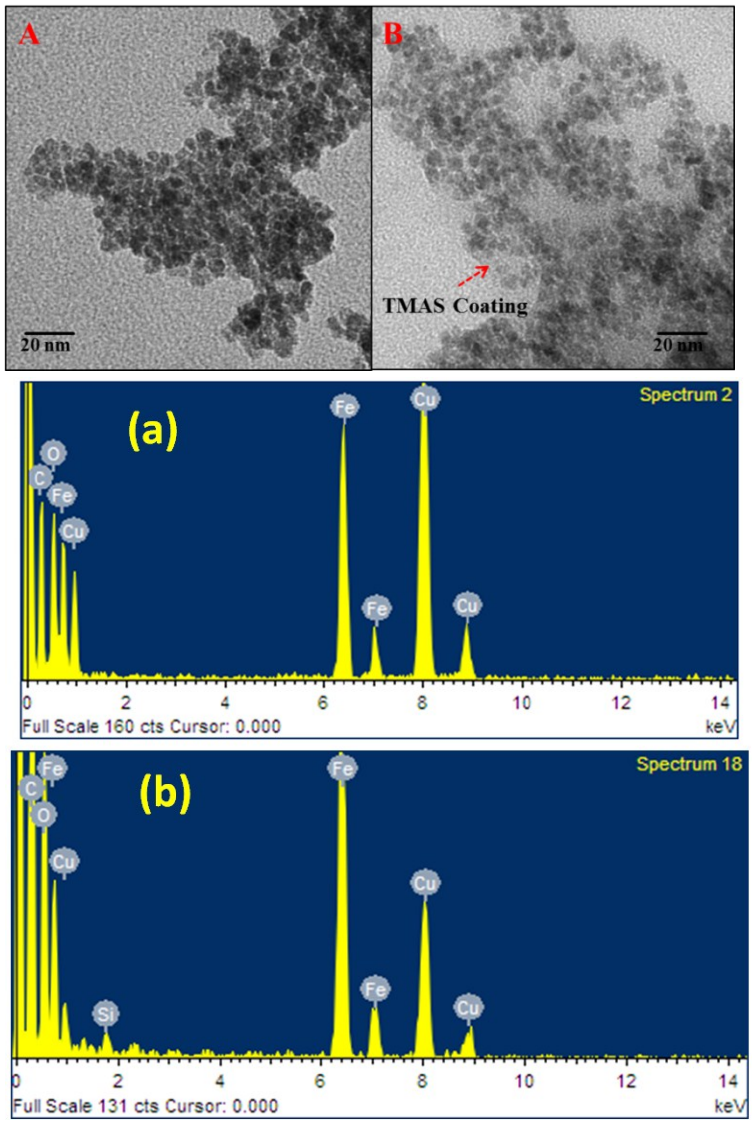

Figure S6: HRTEM micrographs of magnetic Fe_3O_4 nanoparticles (A) before and (B) after coating and EDS spectra of (a) pristine Fe_3O_4 (b) TMAS coated Fe_3O_4

The SAED pattern (Figure S5b) indicates a set of rings instead of spots due to the random orientation of the crystallites, corresponding to reflection planes designated as (220), (311), (400), (422), (511) and (440).

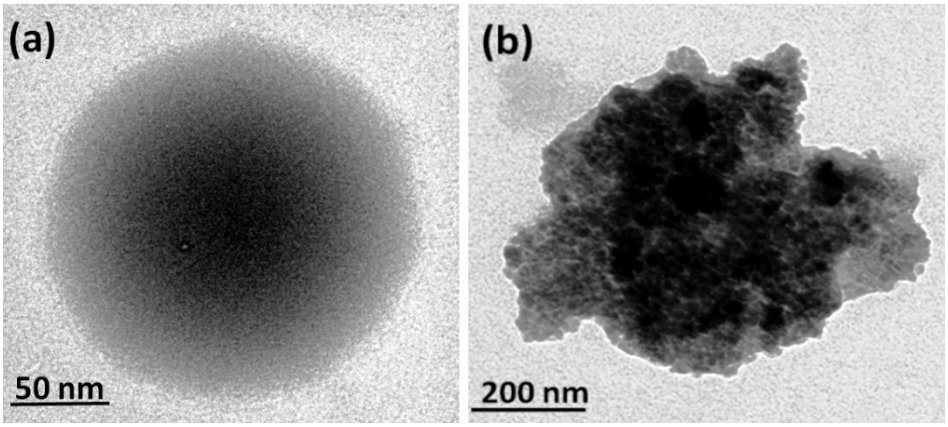

Figure S7: HRTEM image of (a) BCP (PE-P(CL)$_{20}$-b-P(AA)$_{229}$ and (b) nanogel ((PE-P(CL)$_{20}$-b-P(AA)$_{229}$ + 15 wt% TMAS-Fe_3O_4)

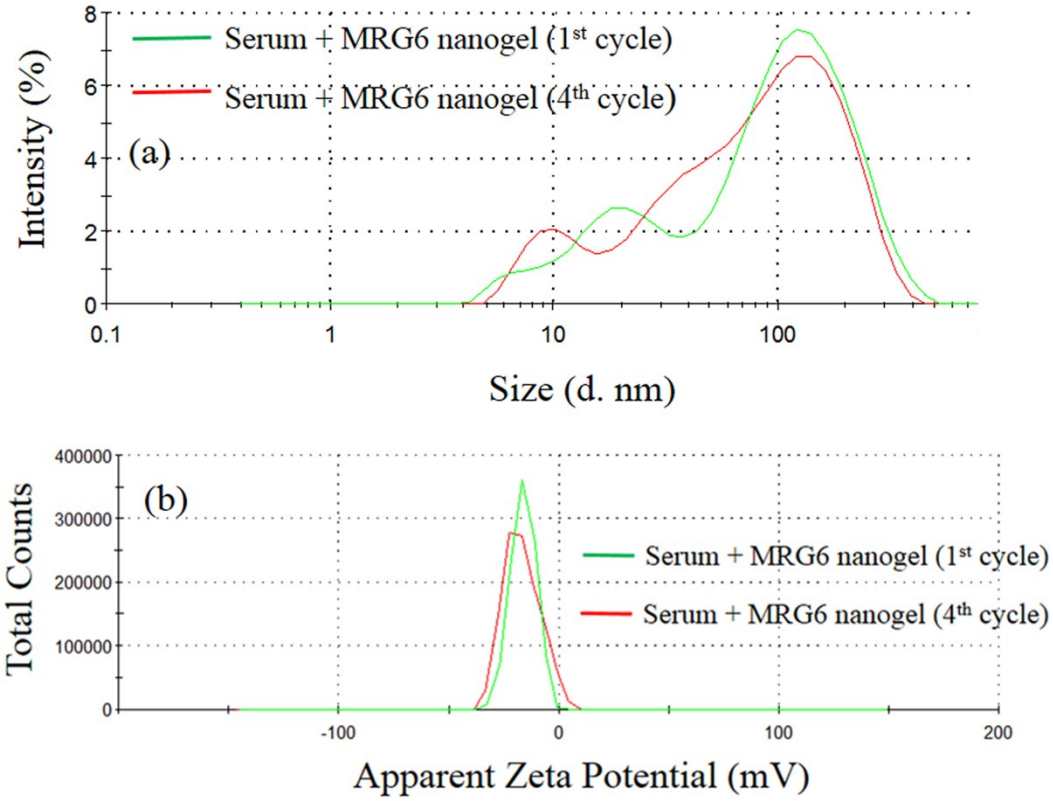

Figure S8 : (a) Size distribution and (b) Zeta potential of MRG6 with serum for 1st and 4th magnetic cycles

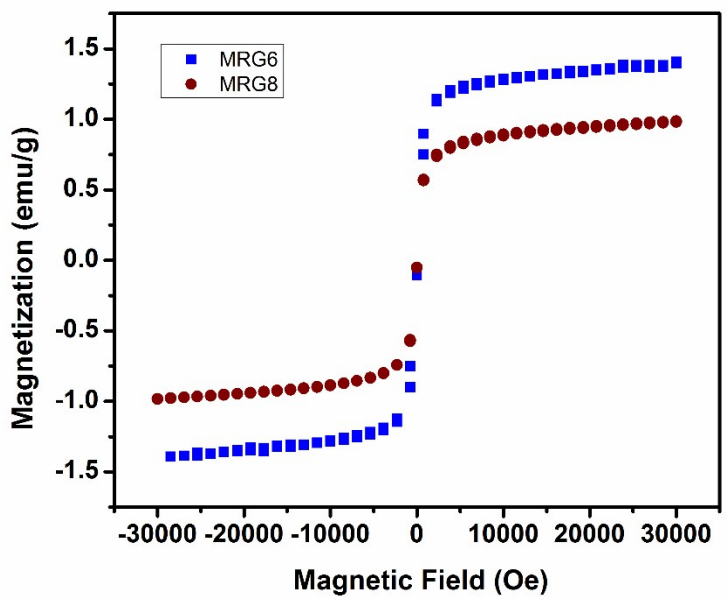

Figure S9: Magnetization versus field (M-H plot) of MRG6 and MRG8

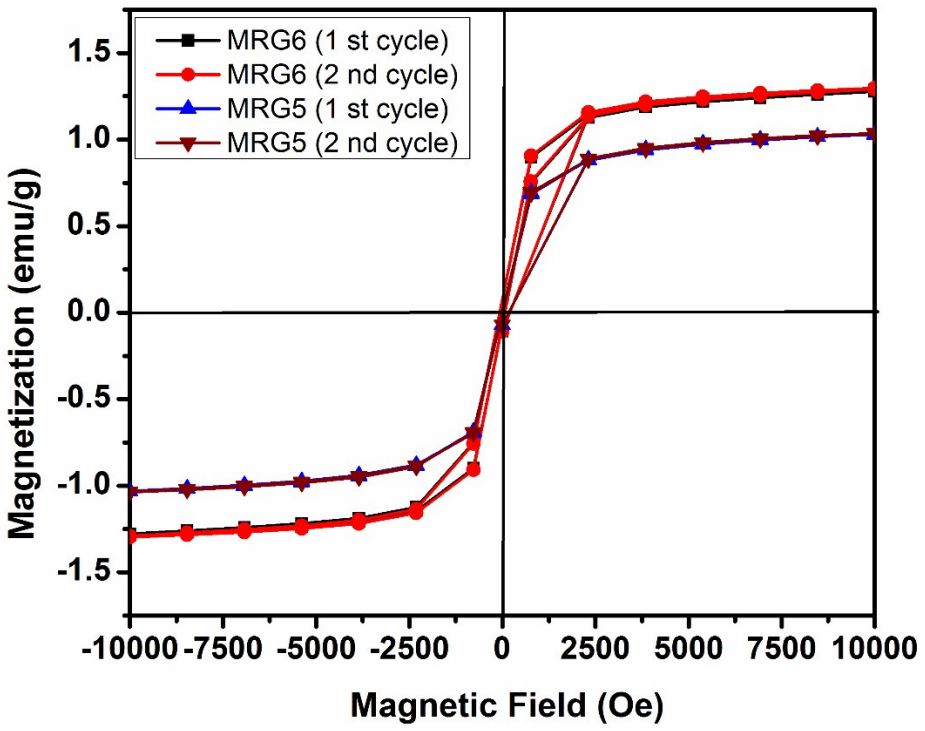

Figure S10: Zoomed view of magnetization versus field (M-H) curve for MRG5 and MRG6

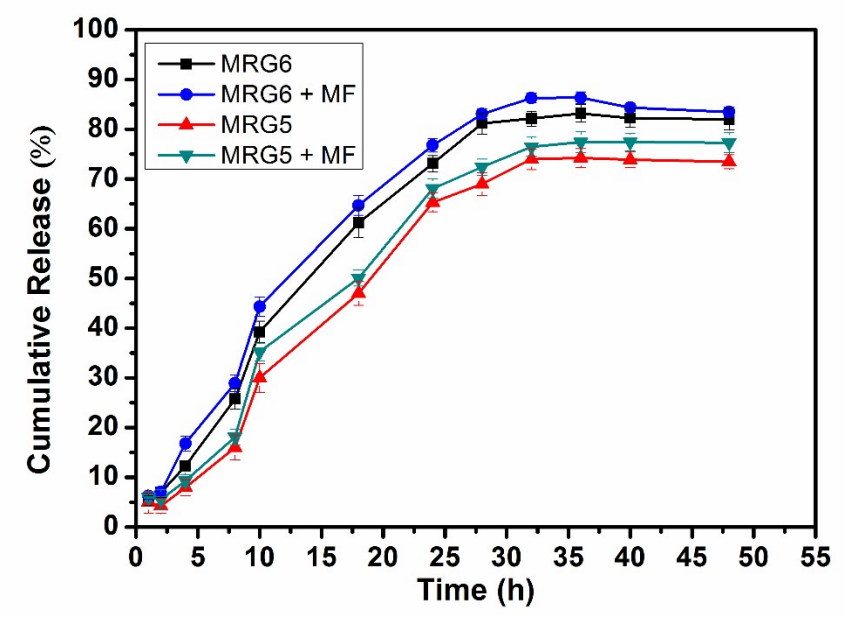

Figure S11: Drug release at pH 5 in presence of static magnetic field

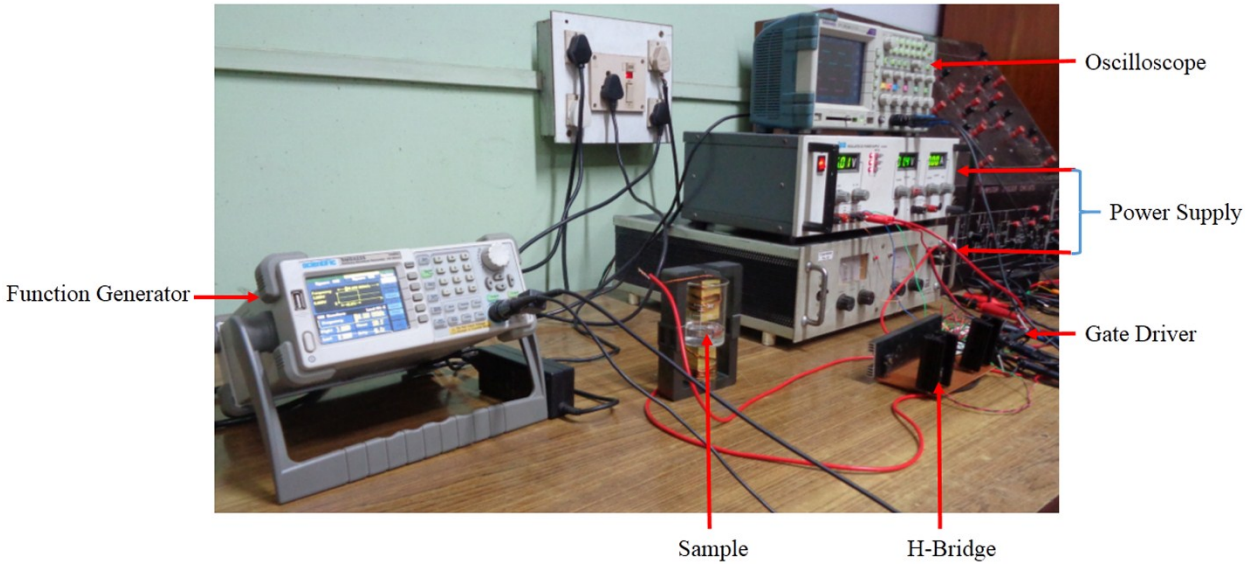

Figure S12: Setup for high frequency alternating magnetic field (HFAMF)

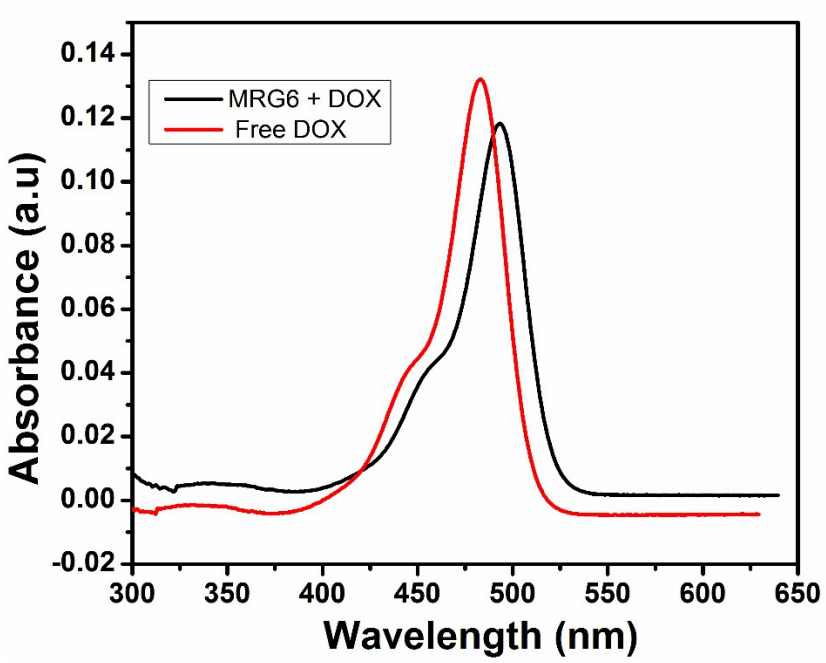

Figure S13: UV absorbance of MRG6 loaded DOX and free DOX

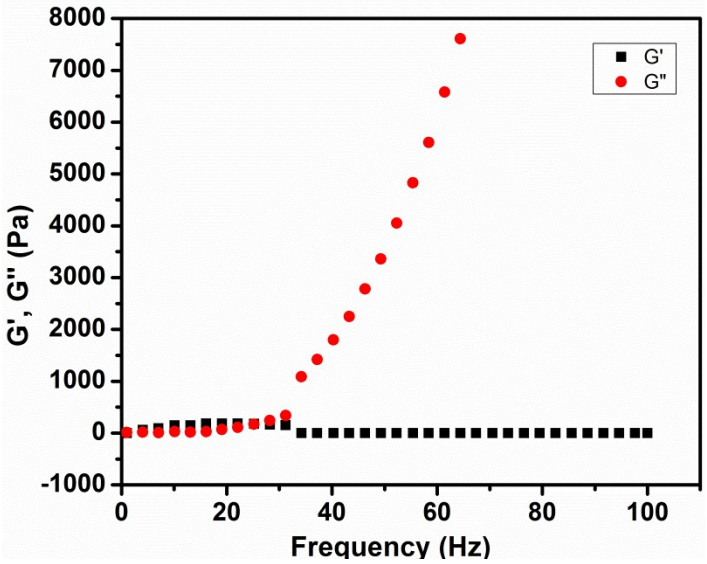

Figure S14: Plot of G' and G" vs. frequency of polymer PE-P$(CL)_{20}$-b-P$(AA)_{180}$ solution

Equation S1:

$$Drug\ loading\ content\ (DLC\ \%) = \frac{Weight\ of\ DOX\ in\ the\ nanogel}{Weight\ of\ the\ nanogel\ taken} \times 100$$

Equation S2:

$$Drug\ loading\ efficiency\ (DLE\ \%) = \frac{Weight\ of\ DOX\ in\ the\ nanogel}{Weight\ of\ the\ DOX\ feeded} \times 100$$

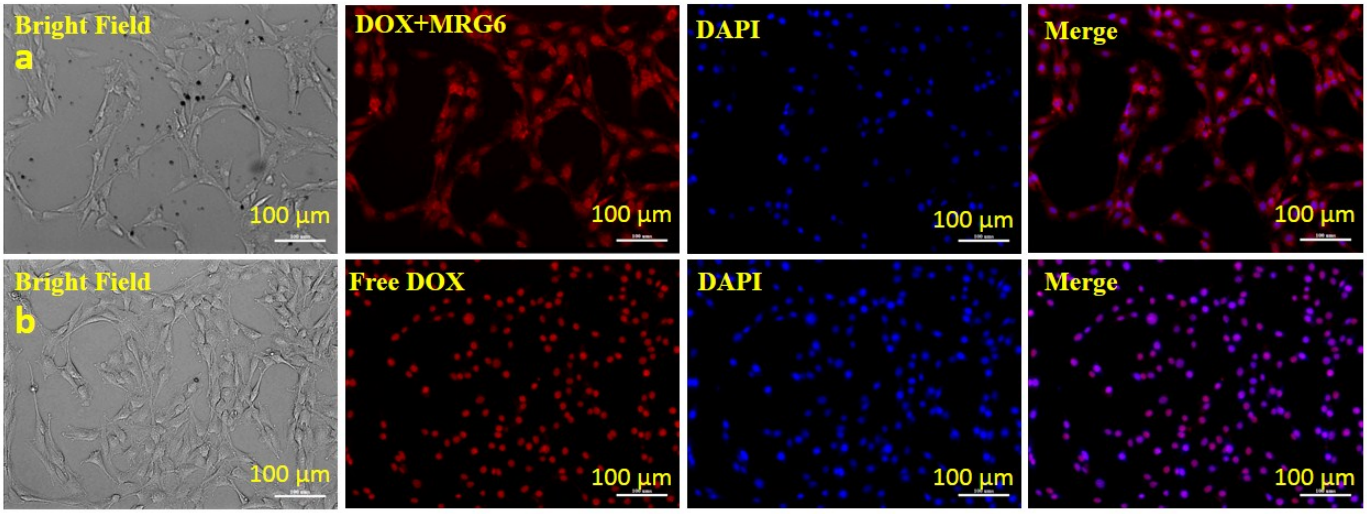

Figure S15: Cell uptake of C6 glioma cell treated with (a) DOX+MRG (b) Free DOX

`

References

1. K. Bogusz, M. Tehei, C. Stewart, M. McDonald, D. Cardillo, M. Lerch, S. Corde, A. Rosenfeld, H. K. Liu and K. Konstantinov, *RSC Adv.*, 2014, **4**, 24412-24419.